ISSN 1330–0008
CODEN FIZAE4

OPTOVOLTAIC SPECTROSCOPY OF A MINIATURE NEON DISCHARGE

DOMAGOJ PAVIČIĆ and DAMIR VEŽA[1]

Institute of Physics, P.O.Box 304, HR-10000 Zagreb, Croatia Tel.: +385-1-4680211

Dedicated to Professor Boran Leontić on the occasion of his 70$^{\mathbf{th}}$ birthday

Received 22 November 1999; Accepted 21 February 2000

We have investigated a miniature radio-frequency–driven neon discharge by means of optovoltaic technique. The optovoltaic signals are induced by a diode laser scanning the neon transition $1s_4 - 2p_7$ (Paschen notation) at 638.3 nm. Our observations suggest that $1s_4$ atoms play a very important role in the generation of optovoltaic signal. The signal-to-noise (S/N) ratio of optovoltaic detection is comparable to the signal-to-noise S/N ratio of the optogalvanic detection.

PACS numbers: 07.62.+s, 33.80.Gj, 35.80.+s,85.60.-q UDC 537.525

Keywords: optogalvanic technique, optovoltaic technique, neon discharge, diode laser spectroscopy

1. Introduction

Compared to the large number of experiments in laser spectroscopy where optogalvanic detection has been used [1], the experiments dealing with the alternative unconventional detection techniques are very rare (examples: [2] on the optovoltaic detection and [3] on the detection of pseudosonic waves). Apparently, there is no reason to neglect such laser spectroscopic techniques, as these methods possess the sensitivity and the signal to noise ratio which are at least comparable to the sensitivity and the signal to noise ratio obtainable by optogalvanic (OG) detection. In order to test the features of the optovoltaic technique we performed a systematic investigation of optovoltaic (OV) effect in a miniature neon discharge. We also compared some OV measurements to OG detection.

[1]veza@ifs.hr; http://www.ifs.hr/~veza

2. *Experimental arrangement*

The discharge source used in this experiment was a miniature neon lamp (see Fig. 1). The discharge was excited either using a high DC voltage to the bulb electrodes (OG measurements), or by a high frequency (RF) field induced by a pair of external, ring-shaped electrodes (OV measurements). In either case we observe a bright, glowing discharge. Although the data about the neon pressure in the bulb are not known, on the basis of the line-shape measurements, we estimate that it should be about 20 mbar at room temperature, giving a room temperature atomic density of about 5×10^{17} cm^{-3}. Since the electron temperature of our RF discharge is about 3 - 5 eV [4], the corresponding electron – neon-atom collision cross-section can be estimated at about 3×10^{-16} cm^2 and electron density at about 10^{10} cm^{-3} [5]. These data lead to an electron – neon-atom collision rate of about 1 GHz and to the Debye length of about 0.1 mm. These features of our RF excited miniature neon discharge represent typical values of a glow discharge plasma.

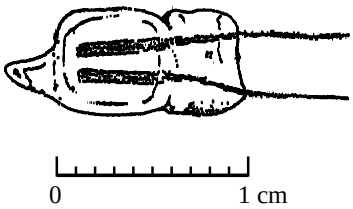

Fig. 1. The miniature neon discharge lamp.

The complete block-diagram of the experimental arrangement is presented in Fig. 2a (optogalvanic measurements) and Fig. 2b (optovoltaic measurements). In the case of optogalvanic measurements, the set-up consisted of a neon lamp connected in series with the current limiting resistor, a stable DC high-voltage source (HV: Stanford Research PS 325), a diode laser (DL), a function generator (FG), a lock-in amplifier (LIA) and a personal computer (PC) equipped with an A/D converter card for data acquisition. The discharge current and the interelectrode potential difference are independently controlled by two digital ampermeters/voltmeters, in order to monitor the corresponding differential resistivity of the investigated neon discharge lamp. The set-up for the optovoltaic experiment consisted of the same miniature neon discharge excited by a RF power supply (RF), a diode laser (DL), a function generator (FG), a lock-in amplifier (LIA) and a PC equipped with an A/D converter card for data acquisition. The discharge was excited with a home made RF-driver [6] based on a 82 MHz oscillator delivering maximum RF power of about 1W (RF-field maximum amplitude unknown). The ring-shaped RF electrodes were made of silvered copper wire (diameter 2 mm) and arranged axially at a distance of about 2.5 cm.

Optical excitation was achieved by a diode laser using a commercial "Hitachi" laser diode (model HL 6316G, $\lambda_0 = 637.1$ nm at room temperature). The signals were excited by tuning the laser to the neon atomic transition $1s_4$ ($^1P_{J=1}$) $\rightarrow$ $2p_7$($^3D_{J=1}$) at 638.3 nm (see Fig. 3). The laser diode was used in the free-running

regime, controlled by the temperature, and the current drivers ("Optima, Inc.", TEC-200 and LDC-202, respectively). The temperature controller can maintain

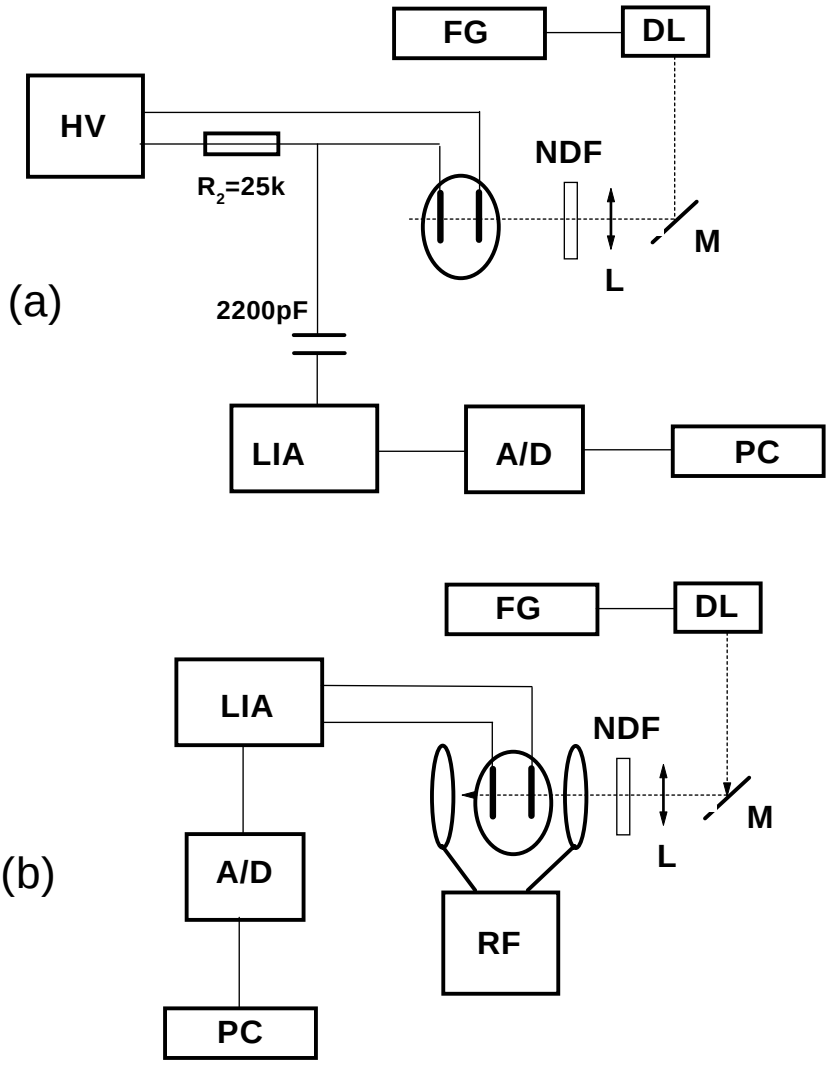

Fig. 2. a) The arrangement of the optogalvanic experiment: HV – *stabilized high-voltage source,* FG – *function generator,* DL – *diode laser,* M – *mirror,* L – *lens,* NDF – *neutral density filter,* LIA – *lock-in amplifier,* A/D – *analog-to-digital converter,* PC – *personal computer. b) The arrangement of the optogalvanic experiment:* RF – *radio-frequency driver, other abbreviations have the same meaning as in a).*

the temperature (here about 37° C) constant to within ±0.005° C. The current driver stabilizes the chosen injection current (here about 30 mA) within $\pm 5\mu$A. The laser diode radiates in a single longitudinal mode, with an estimated linewidth of less than 25 MHz [7,8]. The diode laser system was operated in the constant-current mode, keeping a fixed temperature of the laser diode and slowly sweeping the injection current to scan the neon transition. The sweeping voltage

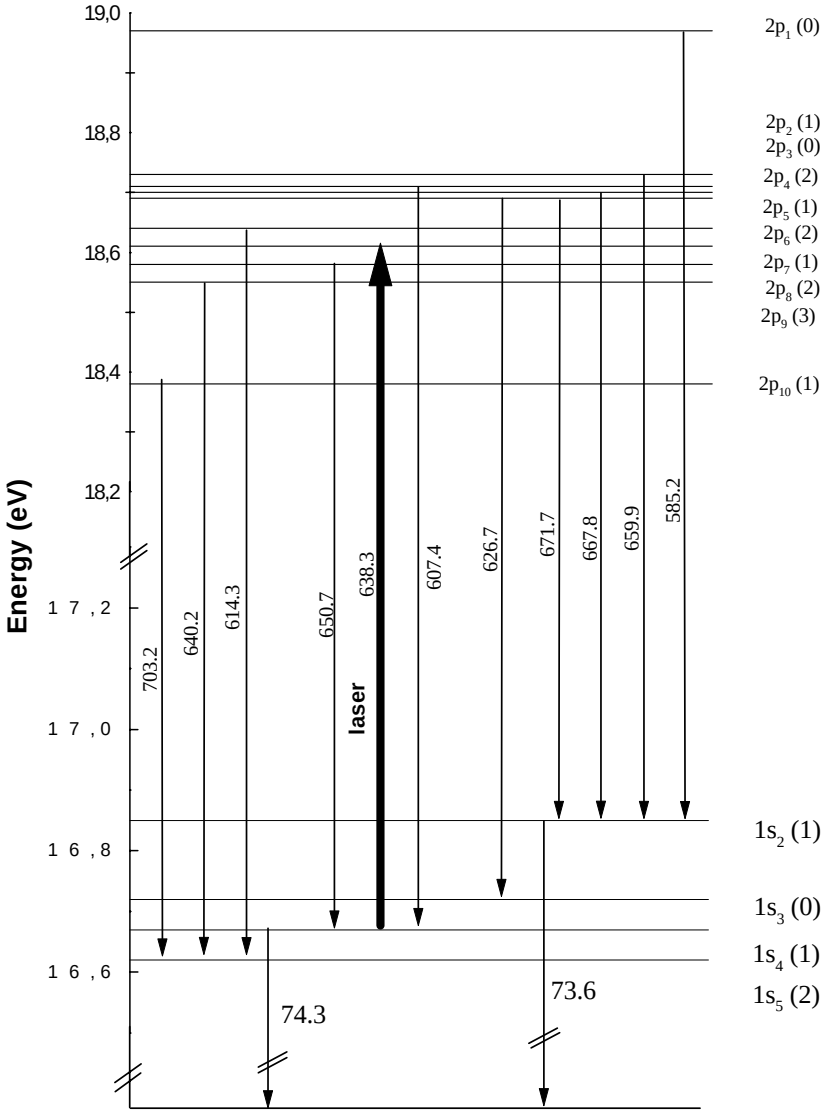

Fig. 3. Partial term diagram of Ne I.

supplied by a function generator is triangular-shaped small amplitude voltage, with scanning frequency of 10 mHz. The scanning range, determined by the sweeping voltage amplitude, was fixed to 10 GHz, thus keeping the same dispersion in each scan. The injection current corresponding to the center excitation wavelength was situated approximately in the middle of a long continuous lasing mode determined by the fixed temperature of the laser diode.

3. Measurements and results

The laser beam was collimated by a long focal length lens to the size of about half a millimeter and directed into the discharge. The lamp was fixed in a holder movable by two micrometer screws, making possible the measurement of OV signals at different lateral laser beam positions in the interelectrode glow region, and the measurements of the same OV signal at different axial bulb positions in the RF field. The OV signal stemming from the optical resonance of laser light with the neon atomic transition was detected via a lock-in amplifier and monitored by an oscilloscope. The OV signal amplified by the lock-in amplifier was digitized using an A/D converter. The second channel of the same A/D converter was used to digitize the wavelength marks. Both signals were stored on the hard disk of a PC for later numerical analysis.

The sign and the width of the observed OV signals are systematically measured at different interelectrode positions of the laser beam and at different positions of the discharge in the RF field. The OV signal-to-noise ratio (S/N) was about 400 in the middle range of chopping frequencies (at about 1 kHz). For comparison, the OG signal-to-noise ratio was about 500. The diode laser intensity was attenuated using neutral density filters, and the power broadening can be neglected in the presented measurements. Since the discharge is excited by a RF field, the bulb electrodes collect the OV signal from the plasmas. The electrodes are spaced about 1.4 mm apart, and the signals were measured in steps of about 0.2 mm starting from the selected bulb electrode (see the inset in Fig. 4). The "selected electrode" is the electrode to which the laser beam is closer [2]. Figure 4 presents the OV signal intensity vs. laser beam position in the interelectrode space for a fixed RF-field intensity. We note that the OV line actually consists of two lines belonging to the ^{22}Ne and the ^{20}Ne isotopes separated by 1685 MHz [9]. The relative isotope abundance ^{22}Ne/^{20}Ne is 0.102 [10]. The numerical analysis [11] reveals a Voigt line shape [12] with about 85% Gaussian fraction [13] in the total line width. The analysis involved fitting a Voigt function, representing the true atomic line shape, to the optovoltaic signal. One such line-profile was fitted to each isotope line. The fitting procedure delivers also the Lorentzian fraction of the total line-width, and knowing the broadening coefficient, $\Delta\nu/N$ [14], one can estimate the corresponding neon collision broadening rate and finally the atomic density. Our estimate is that this neon lamp contains about 20 mbar neon at room temperature.

The maximum signal intensity is reached in the inner points closest to the selected electrode (curves 5 and 11 in Fig. 4), and the signal minimum (almost zero

OV voltage) is reached between the electrodes. Because of the small dimensions of our discharge, the plasma in the vicinity of both bulb electrodes is subjected to the same intensity of the exciting RF field. We can suppose that the electrodes are identical, and "immersed" in the same neon plasma. They are bombarded by electrons, neutral ground state atoms, excited neutral atoms and ions, all of them causing secondary electron emission from the electrodes [2]. The most efficient species are the longest-living and the most energetic ones - the excited neutral neon atoms in $\{1s_i\}$ manifold. The neon metastables (in $1s_5$ and $1s_3$ states) and atoms excited to resonance levels ($1s_4$ and $1s_2$) have by far the largest density (about 10^{13} cm^{-3} according to our measurements [15]) and lifetime (metastables in ms and resonance atoms -because of radiation trapping - in μs to ms range). These atoms, having about 17 eV of internal energy, deactivate upon collision with the electrode surface and eject electrons into the discharge [2]. The electrodes behave as a source of the electromotive force (emf). If the RF field has the same intensity at each electrode, if the electrode areas are equal and have identical surface features, and if the bulb was made symmetrical - the emf voltages generated at the output terminals of the bulb electrodes will be the same; the resulting voltage difference in the outer circuit will be zero. However, if the rate of electron production is changed at one of the electrodes, the emf of this electrode can not balance the emf of the undisturbed electrode. As a consequence, a voltage difference between electrodes will appear. The rate of production of secondary electrons can be decreased, for example, by depleting the $1s_4$ atom population by a laser tuned to the $1s_4$ - $2p_7$ neon transition.

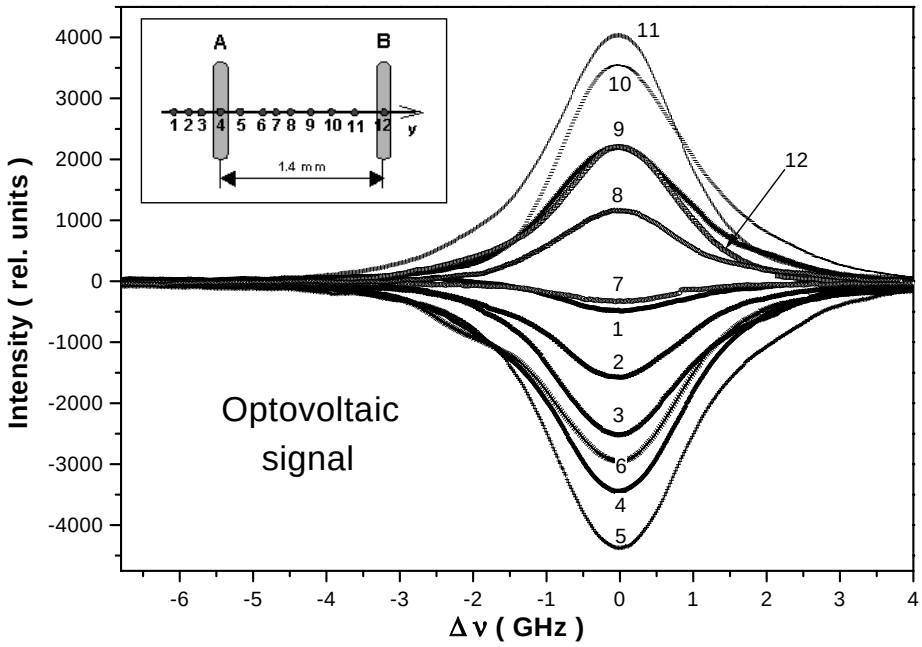

Fig. 4. Intensity and polarity of optovoltaic signal vs. lateral laser beam position (1 to 12) in the glow.

The atoms excited to the $2p_7$ ($J = 1$) atomic state can decay back to any of four $1s_k$ ($k = 0, 1, 2$) levels, proportionally to the level branching ratio. The consequence is that only 62% of all $1s_4$ atoms excited to the $2p_7$ level decay back to $1s_4$ state. The laser-caused $1s_4$ state density change will produce the voltage change (unbalanced emf's) that we measure as the optovoltaic signal [2]. The atoms in the $2p_7$ level can not restore the lowered secondary electron emission because they live to short (ca. 20 ns), and decay before reaching the bulb electrode. Also, the $2p_7$ state with its short level lifetime cannot contribute significantly to the impact ionization in the discharge and cannot compensate the laser induced loss of $1s_4$ atoms.

The OV signals shown in Fig. 4 increase as the laser probes the discharge regions closer to the selected electrode, and decrease in the regions far from the electrodes. Between the electrodes is a point where the laser excitation decreases emf's of both electrodes in a balanced way, producing a negligible OV signal. That point is not exactly in the middle, suggesting that the electrodes and the surface processes are not exactly symmetric. The observations are in agreement with the explanation of the optovoltaic effect given in preceding paragraph.

If the bulb is moved towards one of the RF-electrodes, one can visually observe an increasing brightness of the discharge. The reason is an unbalanced output of our exciter, delivering more RF power to that electrode and, consequently, producing an inhomogeneous RF-field between the electrodes. We also noticed that the bulb is efficiently heated if it is situated near the RF-electrode (at about 1-2 mm distance), where its temperature rises up to about 70° C. The temperature increase and the RF-field inhomogeneity have an influence on the line shape and on the line width. In Fig. 5 we show the intensity of the OV signal vs. the discharge position

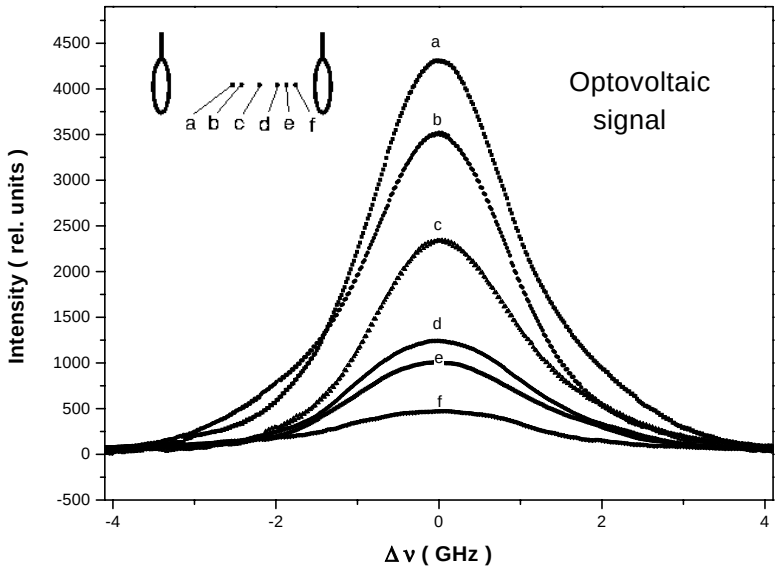

Fig. 5. Intensity of optovoltaic signal vs. axial bulb position ("a" to "f") in the RF field.

in the RF field (positions "a" to "f", see the inset). Surprisingly, the OV signal intensity decreases when the bulb approaches the "stronger" RF electrode and the OV spectral line width increases significantly. One of the reasons for the decreased OV signal intensity can be a decrease of $1s_4$ population by electron or atomic quenching collisions. The decrease of the $1s_4$ population can cause a decrease of the local emf induced by our laser, caused by smaller relative depletion of the $1s_4$ atomic population. In Fig. 6 we plot the total line widths (FWHM of the line profiles measured at positions "a" to "f") and the best fit to the measured data points (the full line). At the bottom of the figure, we show the range of the line-widths of the same atomic line measured with the same lamp using optogalvanic detection. The numerical analysis of optovoltaic line shapes in Fig. 5 reveals the Voigt line shape, with an Lorentzian fraction up to about 15%. However, this calculation alone can not explain the big increase in the total line width, ranging up to 2.6 GHz for the

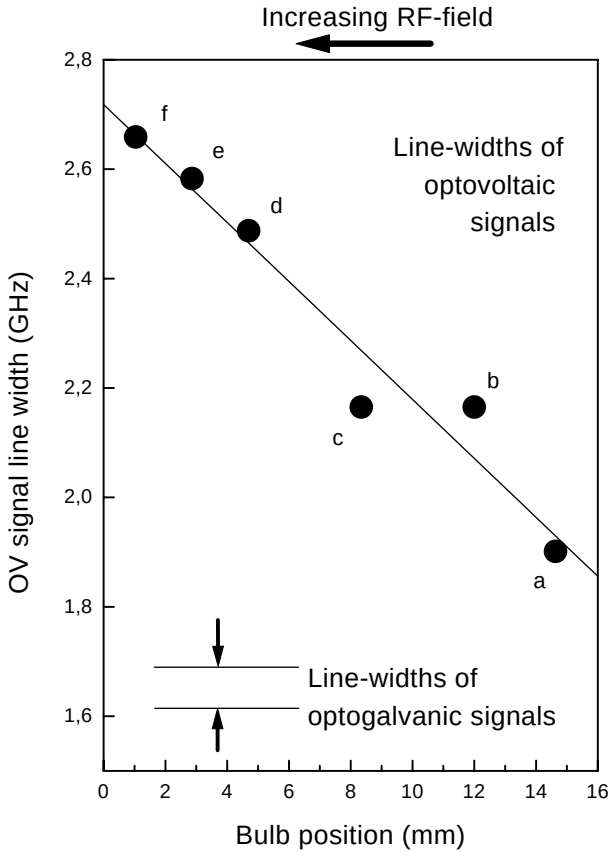

Fig. 6. Line width of optovoltaic signal vs. axial bulb position ("a" to "f") in the RF field. The bulb position is the axial distance of the neon bulb from the RF electrode.

strongest RF fields. We suggest that the large Voigt line widths are caused by a combined effect of increased discharge temperature and the line "smearing" by the strong oscillating RF field. Namely, if we take into account the increase of the bulb temperature observed at points "d", "e" and "f", and the temperature dependence of the collisional and the Doppler broadening, we can reproduce only about 70% of the measured line widths. An additional cause of the line broadening might be the RF-field itself. This field is an oscillating electric field which might affect the $1s_4$ and $2p_7$ neon levels by the Stark shift and Stark splitting [16], resulting in the "smearing" of the atomic line. Unfortunately, the amount of this additional line broadening can not be estimated since the corresponding shift and splitting constants and the peak value of the oscillating RF field are not known.

4. Conclusion

The measurements presented in this paper suggest that the mechanism producing the optovoltaic effect is different from the mechanism causing the optogalvanic effect. Although the leading atomic processes in the discharge and the laser excitation pathway are the same in both cases (optogalvanic as well as in optovoltaic), we have shown that the origin of optovoltaic signal is different. Our measurements show that the optovoltaic line shape and intensity strongly depend not only on the RF-field intensity, but also on the distance of the laser beam from the probe electrode. Concerning the signal-to-noise (S/N) ratio of optovoltaic detection we have found that it is at least comparable to the S/N ratio of the optogalvanic detection.

Acknowledgements

This research was supported by the grant JF107(NIST-IF) of the USA-Croatia Joint Fund for Cooperation in Science and Technology and by the Ministry of Science and Technology of the Republic of Croatia.

References

1) *Int. Coll. Optogalvanic Spect. Appl.*, J. Physique (Suppl.) **C7** (1983); B. Barbieri and N. Beverini, Rev. Mod. Phys. **62** (1990) 603;

2) J. R. Brandenberger, Phys. Rev. **A36** (1987) 76;

3) J. Franzke, M. A. Bratescu, D. Veža and K. Niemax, Mikrochim. Acta **113** (1994) 349;

4) V. Margetić, *Diploma thesis*, Dept. of Physics, University of Zagreb (1997);

5) A. von Engel, *Ionized Gases*, Clarendon Press Oxford (1965);

6) Driver schematics thanks to C. Sansonetti, NIST, Atomic Physics Division, Gaithersburg MD (1997);

7) K. Niemax, H. Groll and C. Schnuerer-Patschan, Spectrochim. Acta. Rev. **15** (1993) 349;

8) J. Franzke, A. Schnell and K. Niemax, Spectrochim. Acta. Rev. **15** (1993) 379;

9) V. I. Odincov, Optika i Spektroskopija **18** (1965) 205; T. Ruhaltinger, *Diplomarbeit*, Techn. Univ. Graz (1988);

10) *CRC Handbook of Chemistry and Physics* 1988 CRC Press, Boca Raton, FL (1988);

11) For numerical analysis we use *The Student Edition of "Matlab"*, Ver. 4, Prentice Hall and The MathWorks Inc., Englewood Cliffs, NJ (1995);
see also http://www.mathworks.com;

12) A. Corney, *Atomic and Laser Spectroscopy*, Clarendon Press, Oxford (1977) Chapt. 8;

13) G. K. Wertheim, M. A. Butler, K. W. West and D. N. E. Buchanan, Rev. Sci. Instrum. **45** (1974) 1369;

14) G. H. Copley, J. Quant. Spectr. Radiat. Transfer **16** (1976) 553;

15) D. Pavičić, *Diploma Work*, Dept. of Physics, University of Zagreb (1999);

16) H. Jaeger and L. Windholz, Phys. Scripta **29** (1984) 344.

OPTOVOLTAIČKA SPEKTROSKOPIJA MALOG IZBOJA U NEONU

Pomoću optovoltaičke metode istraživali smo malen izboj u neonu tjeran radiofrekventnim poljem. Optovoltaički se signali induciraju svjetlom diodnog lasera koje pobuđuje prijelaz $1s_4 - 2p_7$ u neonu (Paschenovo označivanje) na 638.3 nm. Naša opažanja ukazuju da su stanja $1s_4$ vrlo važna u nastajanju optovoltaičkog signala. Omjer signal/šum (S/N) optovoltaičke detekcije je usporediv s omjerom S/N optogalvanske detekcije.